Electronic Supplementary Information

Clinically used antifungal azoles as ligands for gold(III) complexes: the influence of the Au(III) ion on the antimicrobial activity of the complex

Nevena Lj. Stevanović,[a] Jakob Kljun,*[b] Ivana Aleksic,[c] Sanja Skaro Bogojevic,[c] Dusan Milivojevic,[c] Aleksandar Veselinovic,[d] Iztok Turel,*[b] Miloš I. Djuran,*[e] Jasmina Nikodinovic-Runic*[c] and Biljana Đ. Glišić*[a]

[a]*University of Kragujevac, Faculty of Science, Department of Chemistry, R. Domanovića 12, 34000 Kragujevac, Serbia*

[b]*University of Ljubljana, Faculty of Chemistry and Chemical Technology, Večna pot 113, SI-1000 Ljubljana, Slovenia*

[c]*University of Belgrade, Institute of Molecular Genetics and Genetic Engineering, Vojvode Stepe 444a, 11042 Belgrade, Serbia*

[d]*University of Niš, Faculty of Medicine, Department of Chemistry, Blvd. Dr Zorana Đinđića 81, 18108 Niš, Serbia*

[e]*Serbian Academy of Sciences and Arts, Knez Mihailova 35, 11000 Belgrade, Serbia*

*Corresponding authors.

E-mail address: Jakob.Kljun@fkkt.uni-lj.si (J. Kljun); Iztok.Turel@fkkt.uni-lj.si (I. Turel); milos.djuran@pmf.kg.ac.rs (M. I. Djuran); jasmina.nikodinovic@imgge.bg.ac.rs (J. Nikodinovic-Runic); biljana.glisic@pmf.kg.ac.rs (B. Đ. Glišić).

Abstract

In a search for novel antimicrobial metal-based therapeutic agents, mononuclear gold(III) complexes **1–7** of the general formula [$AuCl_3$(azole)], where azole stands for imidazole (im, **1**), 1-isopropylimidazole (ipim, **2**), 1-phenylimidazole (phim, **3**), clotrimazole (ctz, **4**), econazole (ecz, **5**), tioconazole (tcz, **6**) and voriconazole (vcz, **7**) were synthesized, characterized and biologically evaluated. In all complexes, the corresponding azole ligand is monodentately coordinated to the Au(III) *via* the imidazole or triazole nitrogen atom, while the remaining coordination sites are occupied by chloride anions leading to the square-planar arrangement. *In vitro* antimicrobial assays showed that the complexation of inactive azoles, imidazole, 1-isopropylimidazole and 1-phenylimidazole, to the Au(III) ion led to complexes **1–3**, respectively, with moderate activity against the investigated strains and low cytotoxicity on the human normal lung fibroblast cell line (MRC-5). Moreover, gold(III) complexes **4–7** with clinically used antifungal agents clotrimazole, econazole, tioconazole and voriconazole, respectively, have, in most cases, enhanced antimicrobial effectiveness relative to the corresponding azoles, with the best improvement achieved after complexation of tioconazole (**6**) and voriconazole (**7**). The complexes **4–7** and the corresponding antifungal azoles inhibited the growth of dermatophyte *Microsporum canis* at 50 and 25 μg mL^{-1}. Gold(III) complexes **1–3** significantly reduced the amount of ergosterol in the cell membrane of *Candida albicans* at the subinhibitory concentration of 0.5 × MIC (minimal inhibitory concentration), while the corresponding imidazole ligands did not significantly affect the ergosterol content, indicating that the mechanism of action of the gold(III)–azole complexes is associated with inhibition of ergosterol biosynthesis. Finally, complexes **5** and **6** significantly reduced the production of pyocyanin, a virulence factor in *Pseudomonas aeruginosa* controlled by quorum sensing, and increased cell survival after exposure to this bacterium. These findings could

be of importance for the development of novel gold(III)-based antivirulence therapeutic agents that attenuate virulence without pronounced effect on the growth of the pathogens, offering a lower risk for resistance development.

Keywords: Gold(III) complexes; Imidazole; Antifungal azoles; Antimicrobials; *Candida auris*; Quorum sensing

TABLE OF CONTENTS

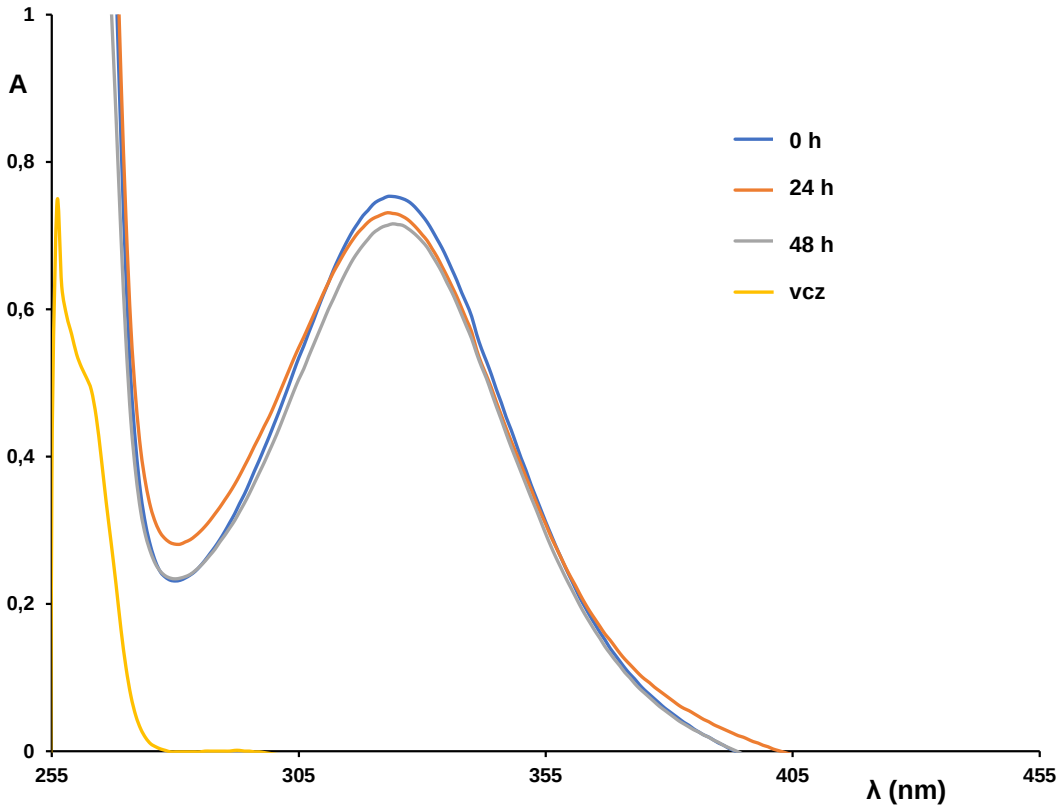

Fig. S1 Stability of the [$AuCl_3$(vcz)] complex (**7**) followed by UV-Vis spectrophotometry at room temperature in DMSO for 48 h. The spectra of vcz ligand recorded in the same solvent was presented for comparison.

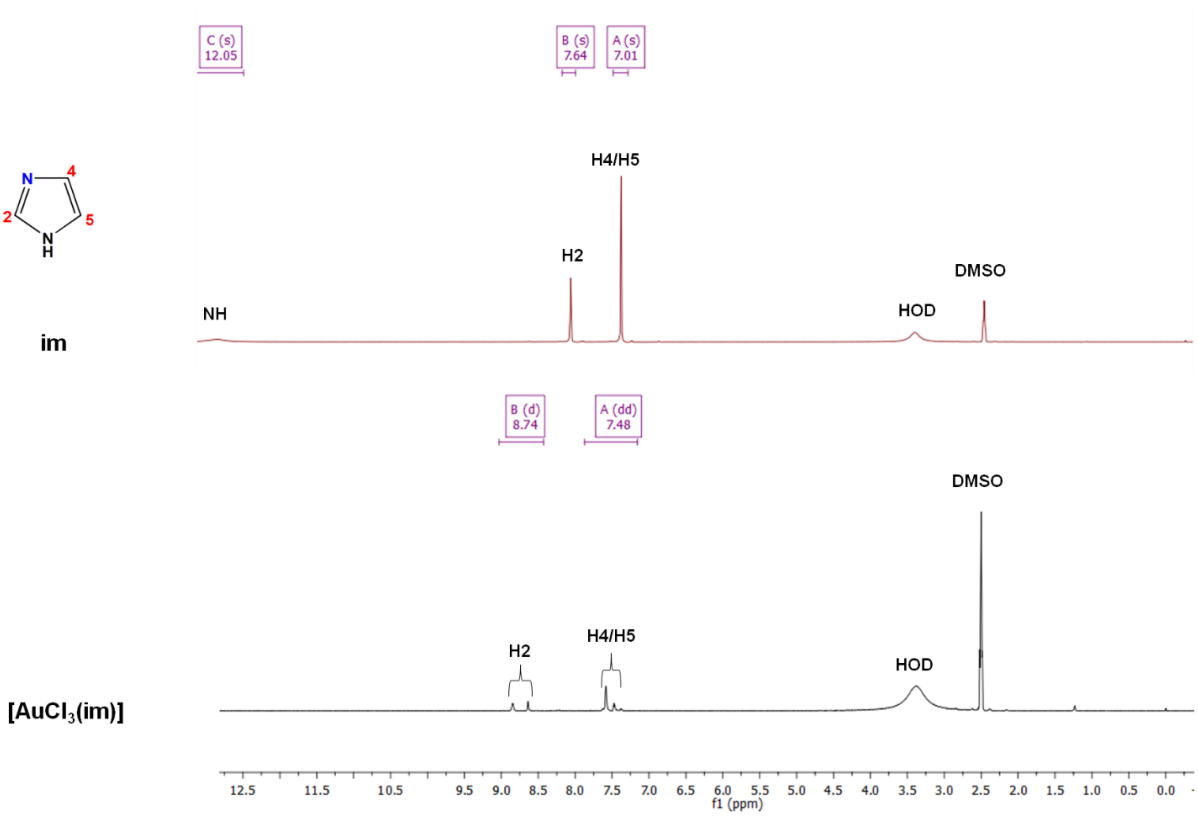

Fig. S2 ^{1}H NMR spectra of imidazole (im) and [$AuCl_3$(im)] **(1)** (DMSO, 200 MHz).

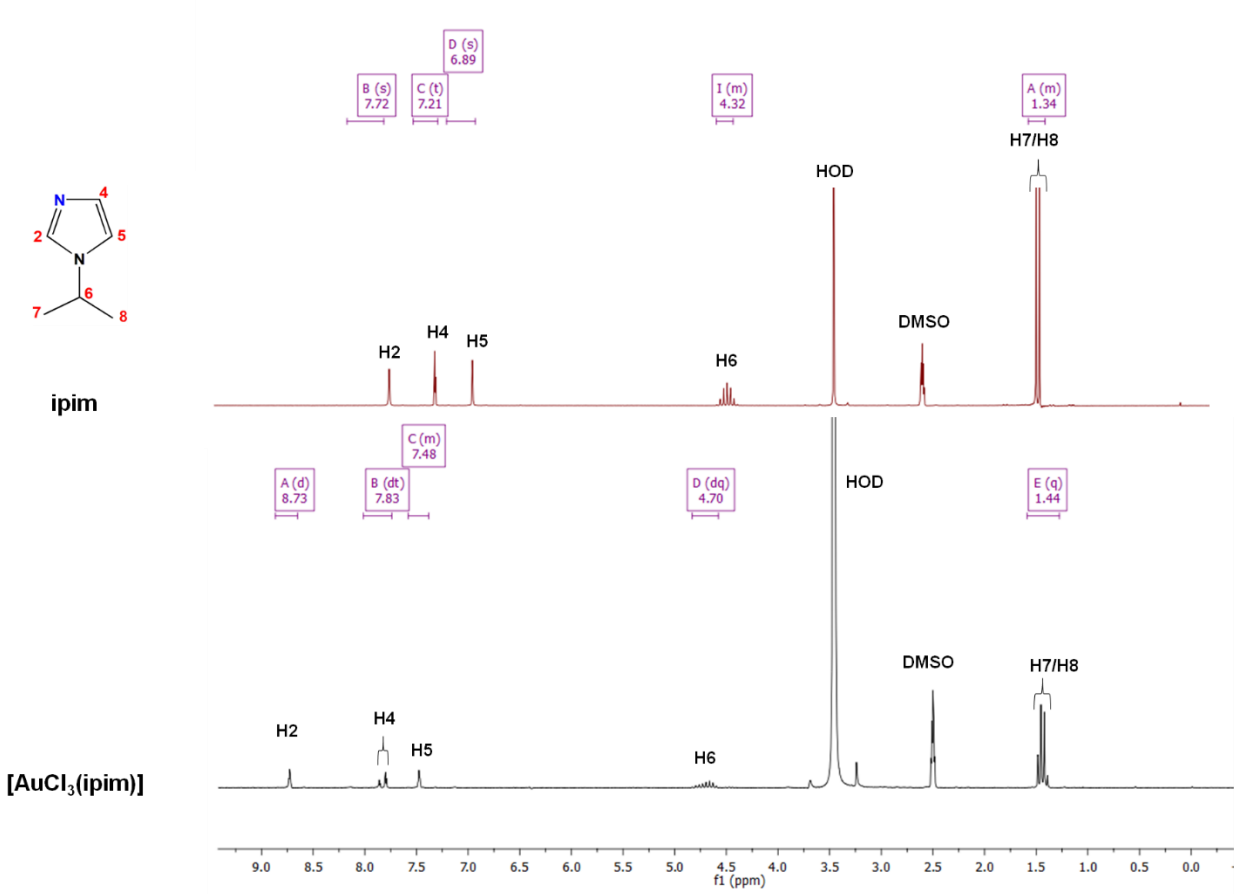

Fig. S3 ^{1}H NMR spectra of 1-isopropylimidazole (ipim) and [$AuCl_3$(ipim)] **(2)** (DMSO, 200 MHz).

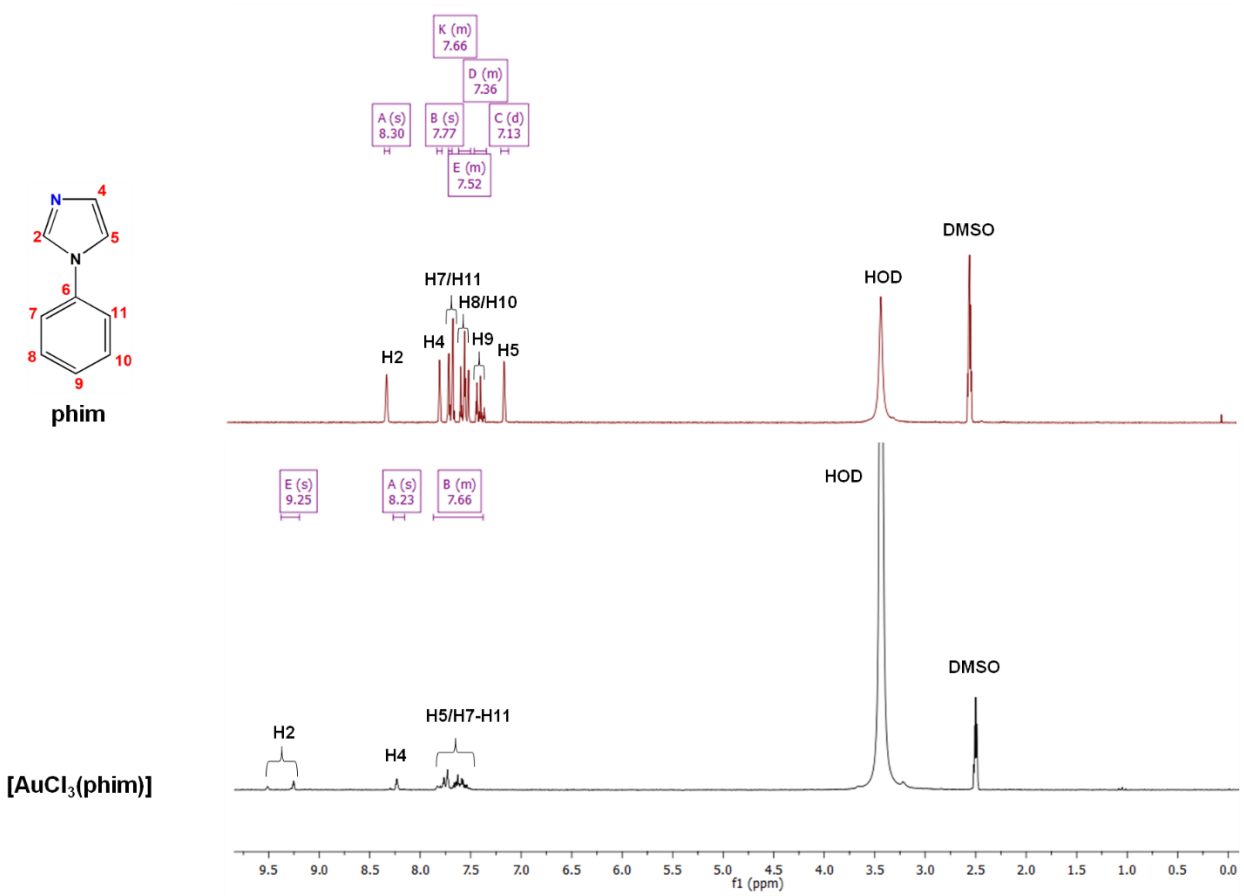

Fig. S4 ^{1}H NMR spectra of 1-phenylimidazole (phim) and [$AuCl_3$(phim)] **(3)** (DMSO, 200 MHz).

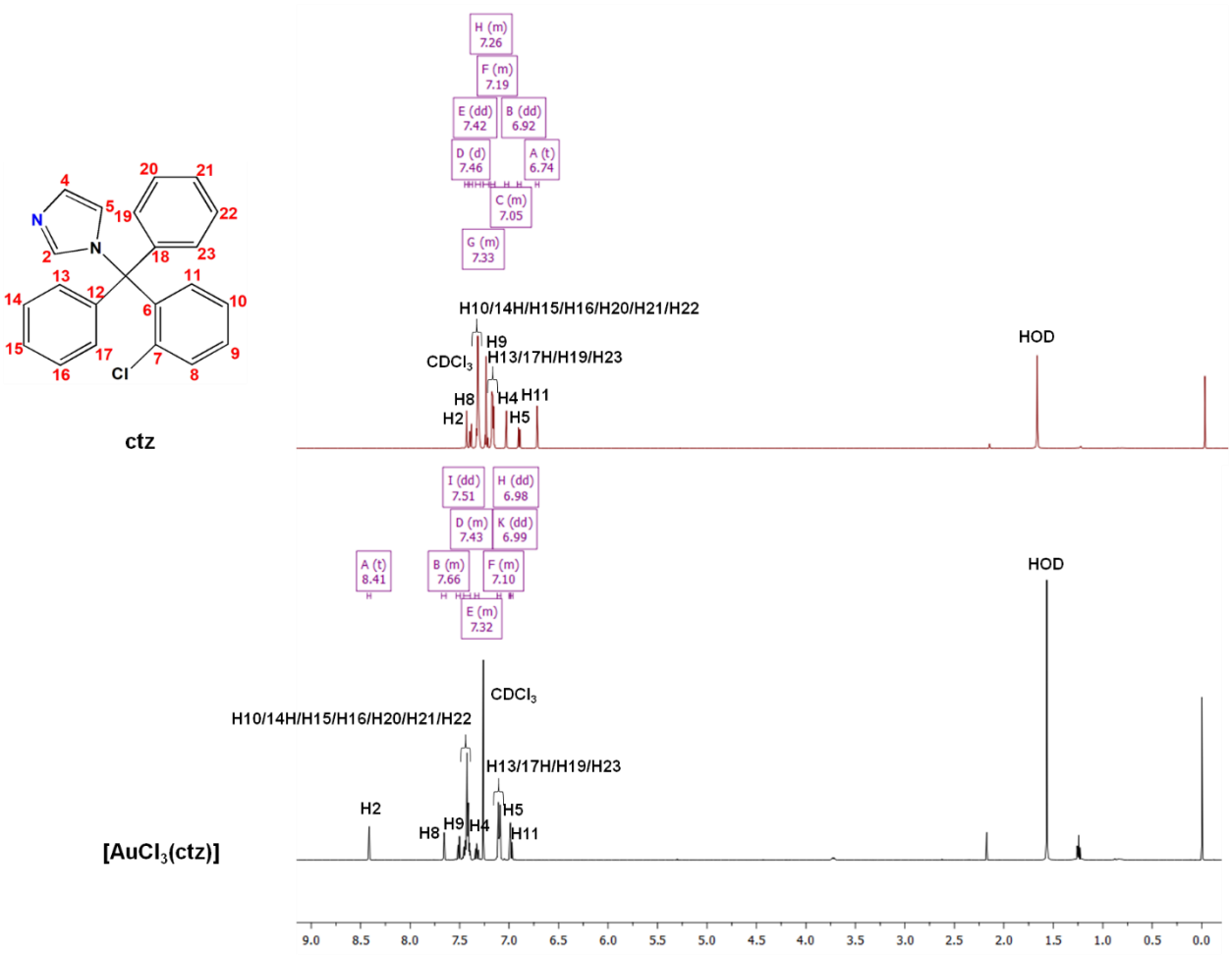

Fig. S5 ^{1}H NMR spectra of clotrimazole (ctz) and [$AuCl_3$(ctz)] **(4)** ($CDCl_3$, 500 MHz).

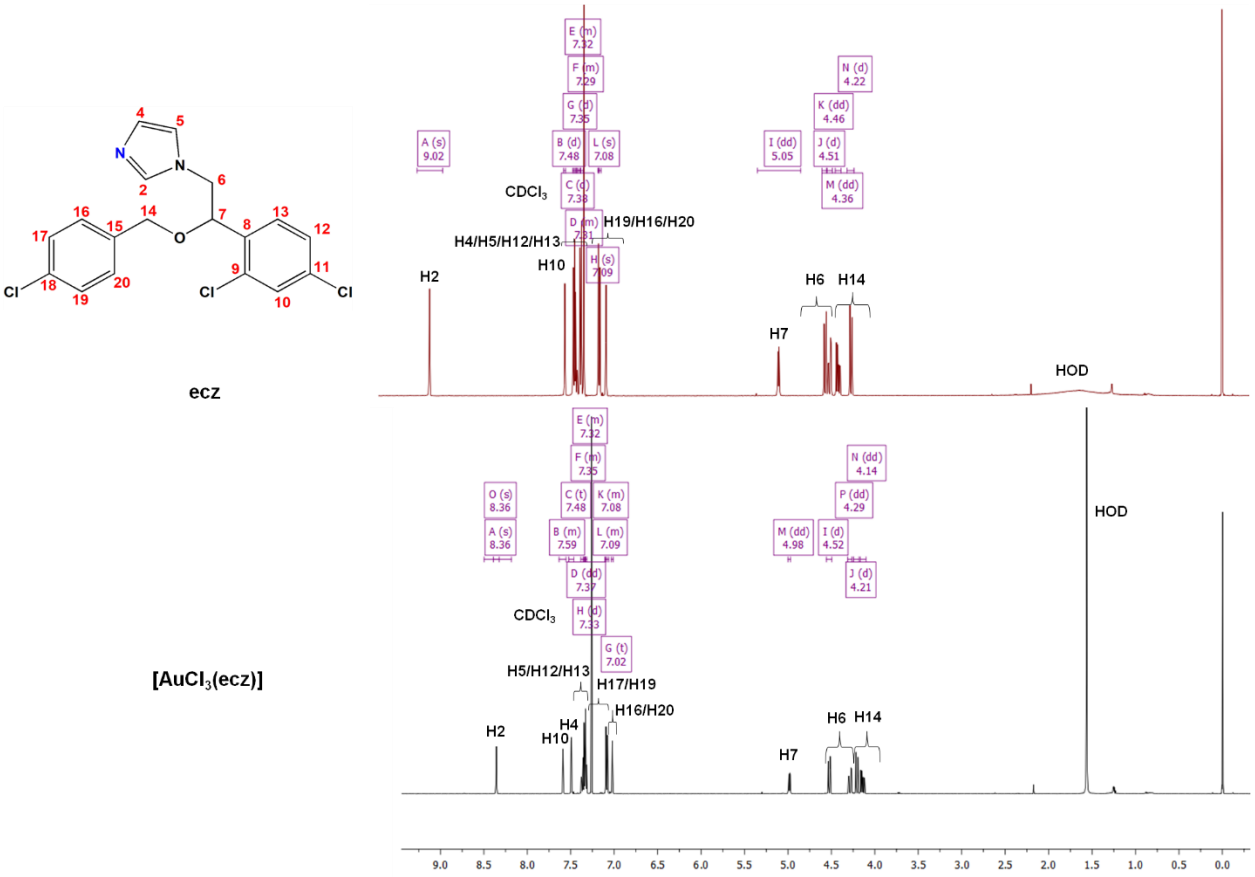

Fig. S6 ^{1}H NMR spectra of econazole (ecz) and [$AuCl_3$(ecz)] **(5)** ($CDCl_3$, 500 MHz).

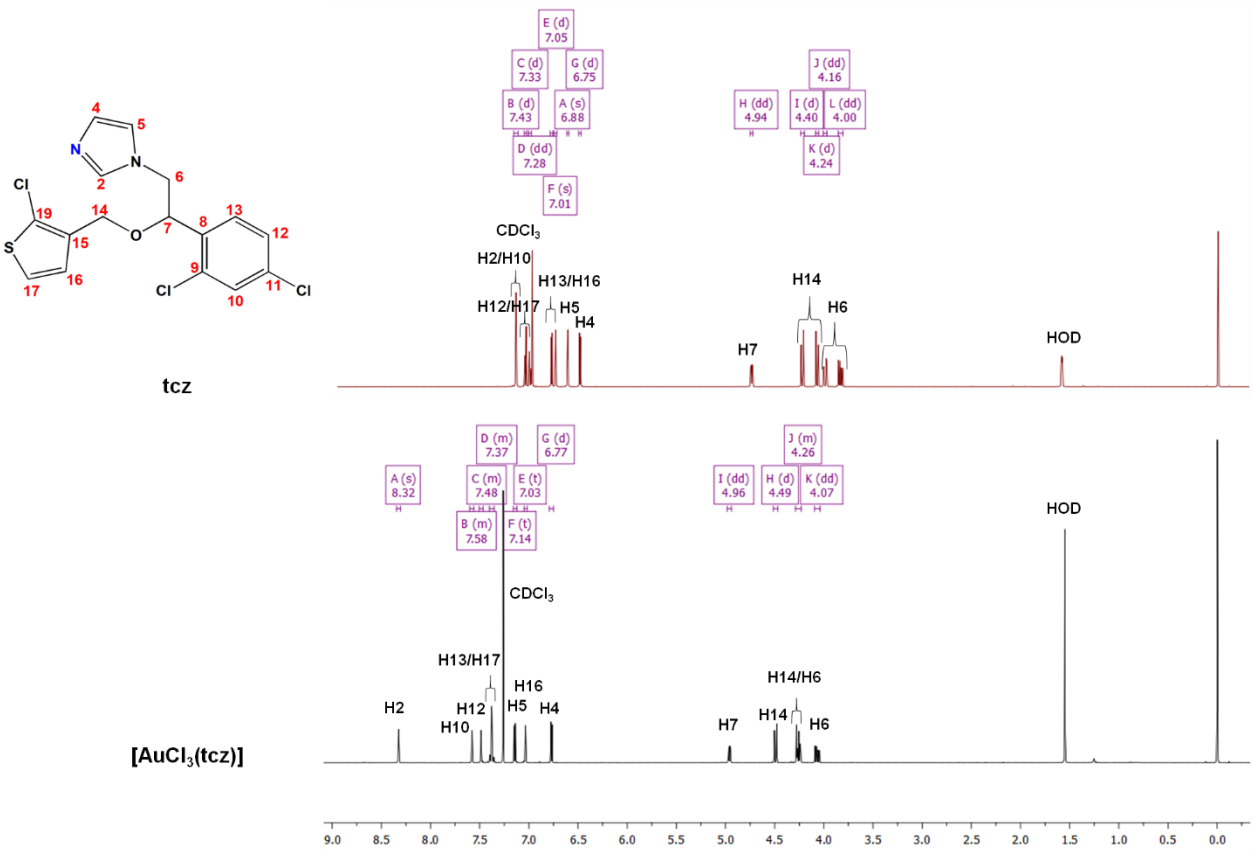

Fig. S7 ^{1}H NMR spectra of tioconazole (tcz) and [$AuCl_3$(tcz)] **(6)** ($CDCl_3$, 500 MHz).

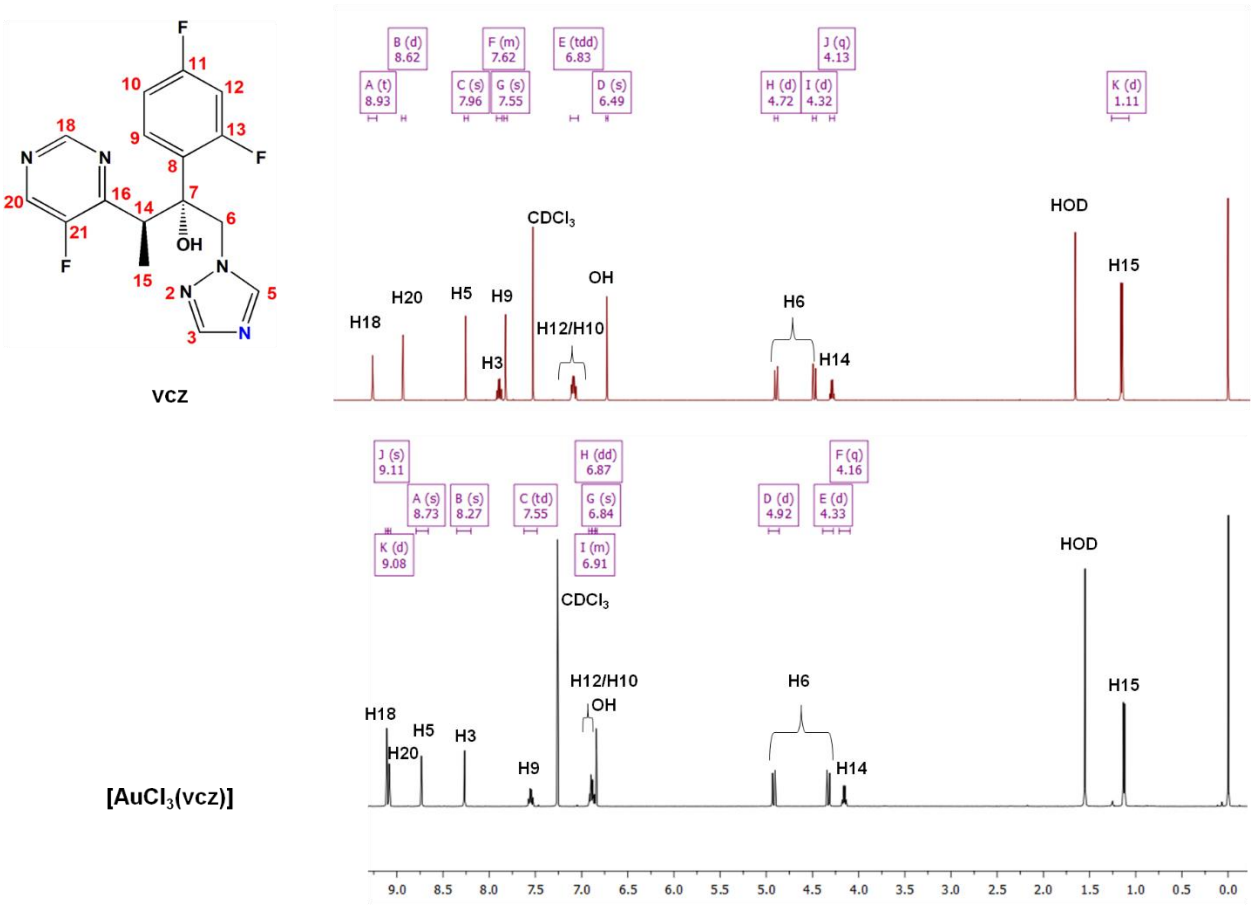

Fig. S8 ^{1}H NMR spectra of voriconazole (vcz) and [$AuCl_3$(vcz)] **(7)** ($CDCl_3$, 500 MHz).

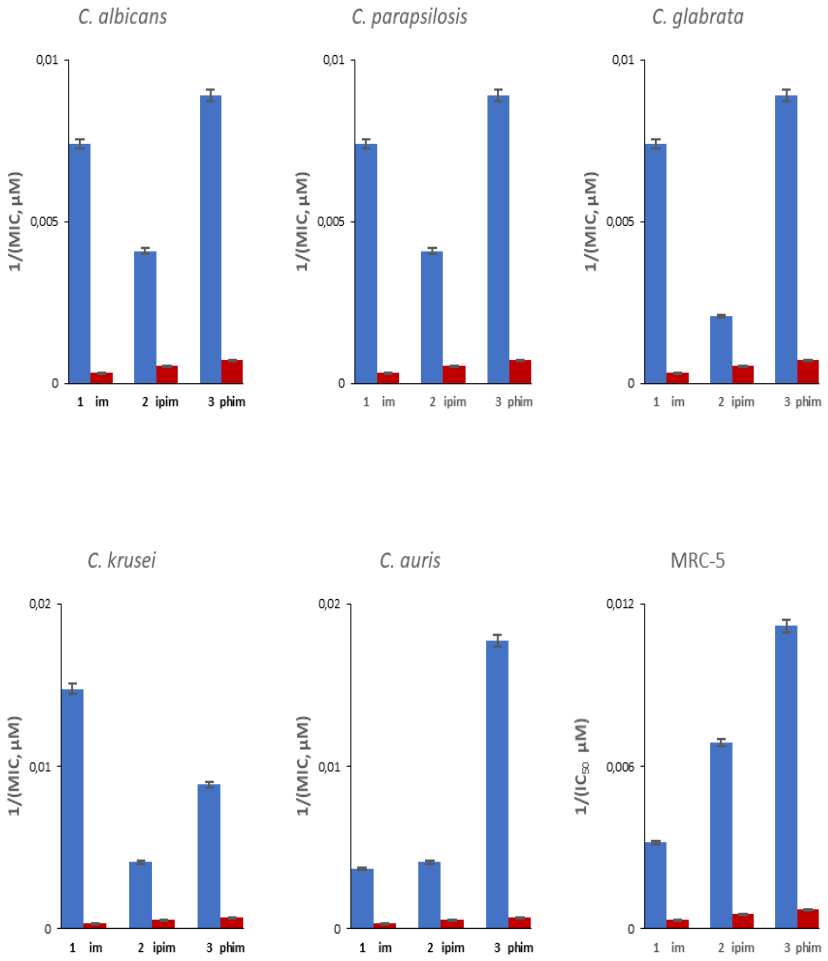

Fig. S9 Graphical illustration of the antifungal (1/(MIC, µM)) and antiproliferative activity ($1/IC_{50}$, µM) of gold(III) complexes **1 – 3** and the corresponding non-antifungal azoles against the selection of *Candida* strains.

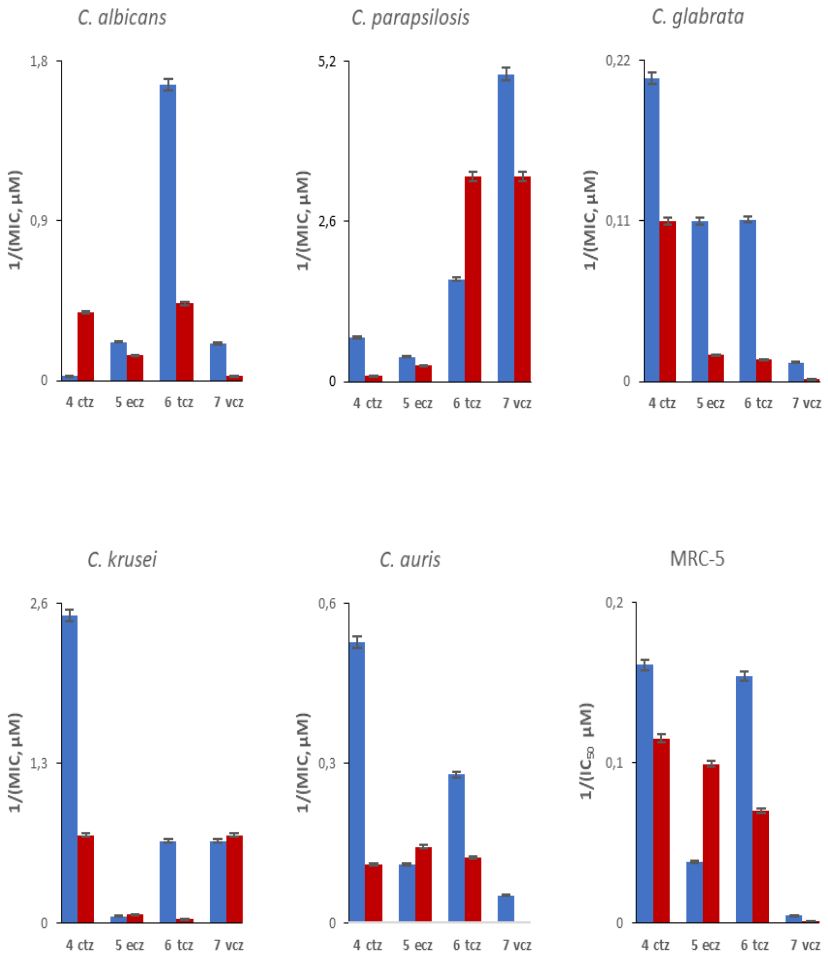

Fig. S10 Graphical illustration of the antifungal (1/(MIC, µM)) and antiproliferative activity ($1/IC_{50}$, µM) of gold(III) complexes **4 – 7** and the corresponding clinically used azoles against the selection of *Candida* strains.

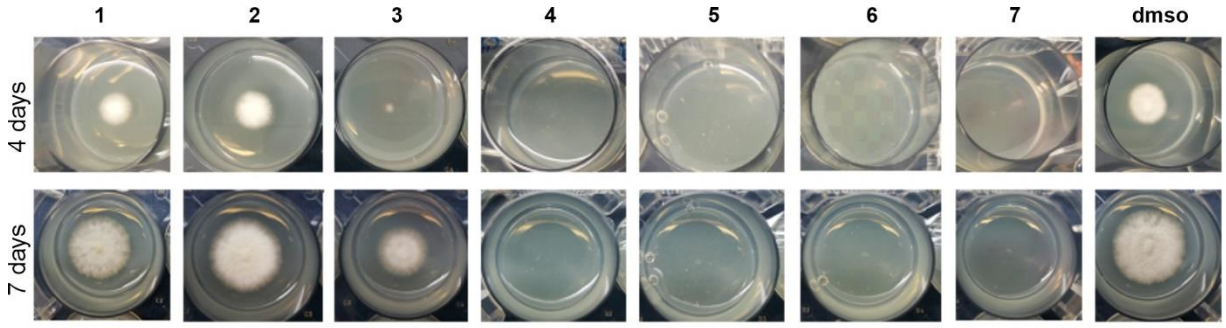

Fig. S11 Inhibition of *Microsporum canis* by gold(III) complexes **1 – 7**. 50 µg mL^{-1} of compounds was added to the medium prior to solidification.

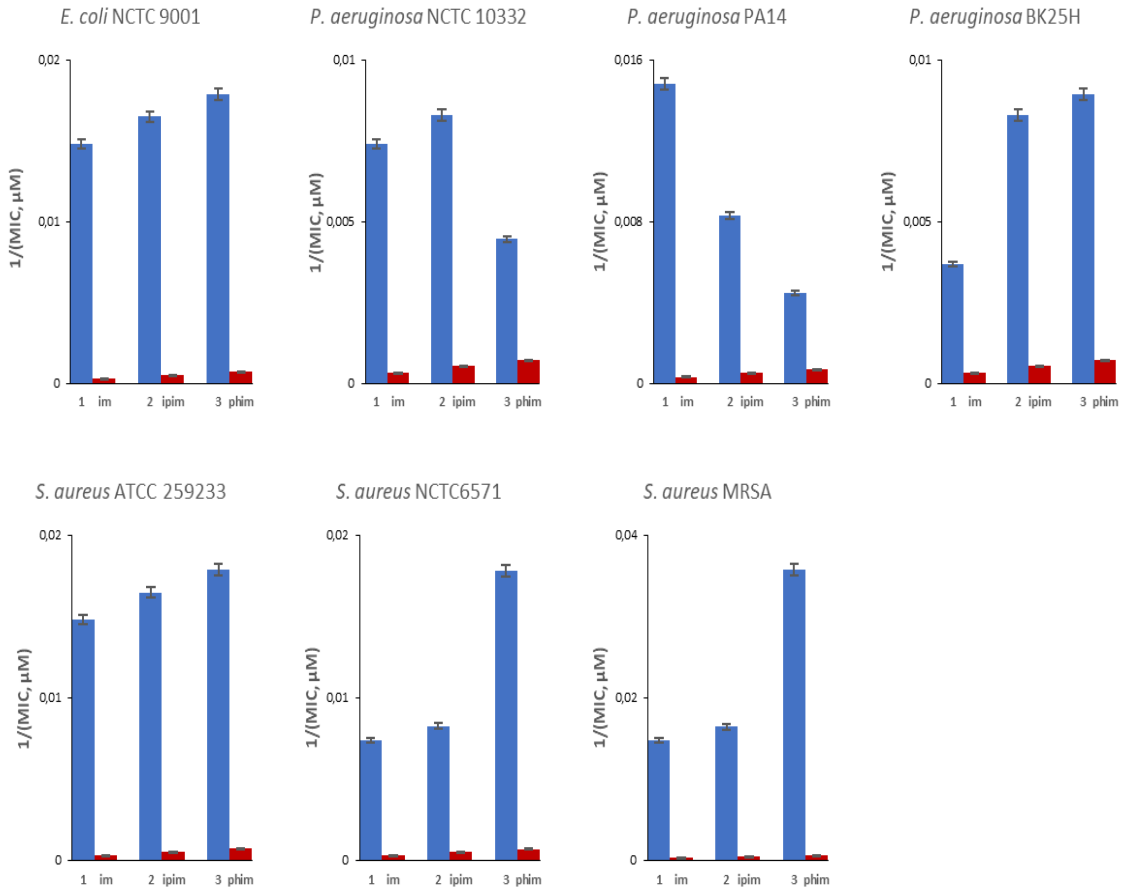

Fig. S12 Graphical illustration of antibacterial activity (1/(MIC, μM)) of gold(III) complexes **1** – **3** and the corresponding non-antifungal azoles against the selection of bacterial strains.

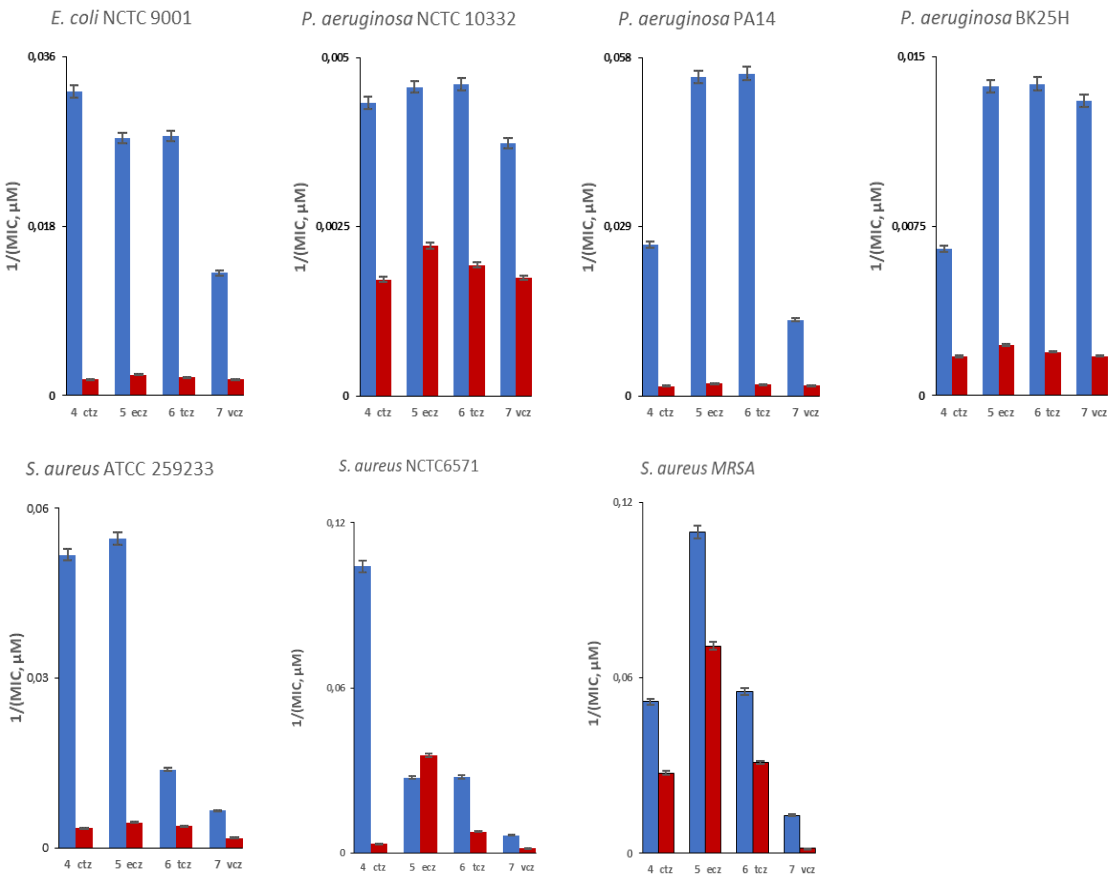

Fig. S13 Graphical illustration of antibacterial activity (1/(MIC, μM)) of gold(III) complexes **4 – 7** and the corresponding azoles against the selection of bacterial strains.

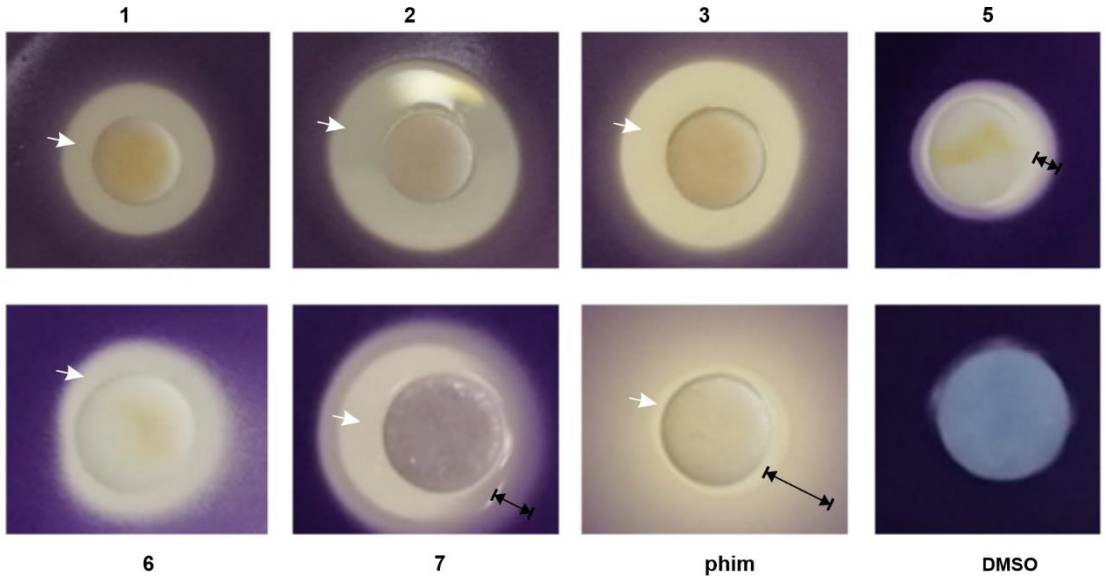

Fig. S14 Inhibition of violacein production in the presence of gold(III)-azole complexes **1 – 3**, **5 – 7** and ligand phim tested on *Chromobacterium violaceum* CV026 at 200 µg per disc concentration. White arrows denote zones of growth inhibition and black measuring lines indicate zones of violacein synthesis inhibition. DMSO was used as solvent control.

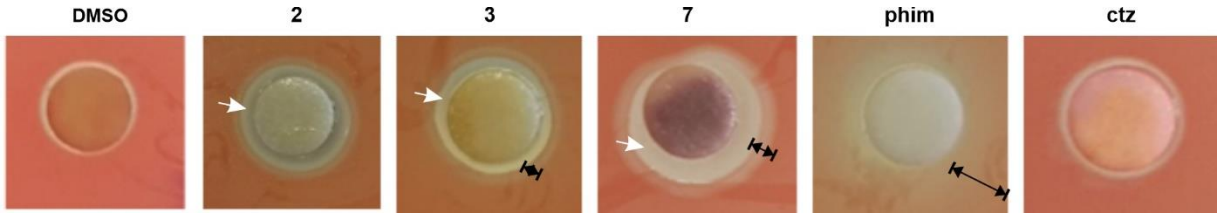

Fig. S15 Inhibition of prodigiosin production in the presence of gold(III)-azole complexes **2, 3, 7** and ligand phim and ctz tested on *Serratia marcescens* at 200 µg per disc concentration. White arrows denote zones of growth inhibition and black measuring lines indicate zones of prodigiosin synthesis inhibition. DMSO was used as solvent control.

Table S1 The selectivity index value (SI) of gold(III)-azole complexes **1 – 7** and the azole ligands on *Candida* strains

Test organism / Au(III) complex/azole	*C. albicans* ATCC 10231	*C. parapsilosis* ATCC 22019	*C. glabrata* ATCC 2001	*C. krusei* ATCC 6258	*C. auris* ATCC 21092
Au(III) complex/Imidazole					
$[AuCl_3(im)]$ **(1)**	2.3	2.3	2.3	4.6	1.1
imidazole (im)	n/a[a]	n/a	n/a	n/a	n/a
$[AuCl_3(ipim)]$ **(2)**	0.6	0.6	**0.3**	0.6	0.6
1-isopropylimidazole (ipim)	n/a	n/a	n/a	n/a	n/a
$[AuCl_3(phim)]$ **(3)**	0.8	0.8	0.8	0.8	1.6
1-phenylimidazole (phim)	n/a	1	1	1	n/a
Au(III) complex/Clinically used azole					
$[AuCl_3(ctz)]$ **(4)**	**0.2**[b]	4.4	1.3	15.5	3.3
clotrimazole (ctz)	3.3	0.8	1	6.2	1
$[AuCl_3(ecz)]$ **(5)**	5.7	10.5	2.9	1.4	2.9
econazole (ecz)	1.4	2.6	**0.2**	0.7	1.4
$[AuCl_3(tcz)]$ **(6)**	10.8	10.8	0.7	4.3	1.8
tioconazole (tcz)	6.2	47.3	**0.2**	0.4	1.7
$[AuCl_3(vcz)]$ **(7)**	44.8	**1075**	2.8	143.3	11.2
voriconazole (vcz)	24	**2863**	1.5	**613**	1.5

[a]not applicable, as compounds were not cytotoxic in the concentrations tested;
[b]the highest and the lowest (not so favorable) values are marked in bold.

Table S2 Crystallographic data for complexes **3 – 5** and **7**

Compound	**3**	**4**
CCDC No.	2099556	2099557
Empirical formula	$C_9H_8AuCl_3N_2$	$C_{22}H_{17}AuCl_4N_2$
Formula weight	447.49	648.14
Temperature/K	150.00(10)	150.00(10)
Crystal system	monoclinic	monoclinic
Space group	$P2_1/n$	$P2_1/n$
a/Å	8.7297(5)	9.4310(4)
b/Å	6.9516(3)	18.1660(7)
c/Å	19.7326(11)	12.7936(6)
α/°	90	90
β/°	102.008(5)	100.300(4)
γ/°	90	90
Volume/Å^3	1171.28(11)	2156.52(16)
Z	4	4
ρ_{calc} g cm^{-3}	2.538	1.996
μ/mm^{-1}	13.210	7.329
F(000)	824.0	1240.0
Crystal size/mm^3	0.3 × 0.05 × 0.05	0.6 × 0.5 × 0.4
Radiation	Mo Kα (λ = 0.71073)	Mo Kα (λ = 0.71073)
2Θ range for data collection/°	4.7704 to 58.8898	4.93 to 51.362
Index ranges	-10 ≤ h ≤ 11, -9 ≤ k ≤ 9, -24 ≤ l ≤ 24	-11 ≤ h ≤ 11, -21 ≤ k ≤ 22, -11 ≤ l ≤ 15
Reflections collected	8011	13267
Independent reflections	2782 [R_{int} = 0.0316, R_{sigma} = 0.0467]	4091 [R_{int} = 0.0247, R_{sigma} = 0.0242]
Data/restraints/parameters	2782/0/136	4091/0/262
Goodness-of-fit on F^2	1.057	1.055
Final R indexes [I ≥ 2σ (I)]	R_1 = 0.0280, wR_2 = 0.0603	R_1 = 0.0231, wR_2 = 0.0535
Final R indexes [all data]	R_1 = 0.0359, wR_2 = 0.0656	R_1 = 0.0289, wR_2 = 0.0561
Largest diff. peak/hole / e Å^{-3}	1.93/-2.15	1.06/-1.08
Flack parameter	/	/

Continuation of Table S2.

Compound	**5**	**7**
CCDC No.	2099558	2099560
Empirical formula	$C_{18}H_{15}AuCl_6N_2O$	$C_{16}H_{14}AuCl_3F_3N_5O$
Formula weight	684.99	652.64
Temperature/K	150.05(10)	150.00(10)
Crystal system	triclinic	monoclinic
Space group	P-1	$P2_1$
a/Å	7.5671(3)	12.1573(5)
b/Å	9.5470(5)	5.8115(2)
c/Å	15.8505(7)	15.0653(6)
α/°	89.941(4)	90
β/°	80.989(4)	99.973(4)
γ/°	76.380(4)	90
Volume/Å^3	1098.39(9)	1048.32(7)
Z	2	2
ρ_{calc} g cm^{-3}	2.071	2.068
μ/mm^{-1}	7.439	7.443
F(000)	652.0	620.0
Crystal size/mm^3	0.2 × 0.2 × 0.1	0.3 × 0.05 × 0.05
Radiation	Mo Kα (λ = 0.71073)	MoKα (λ = 0.71073)
2Θ range for data collection/°	5.208 to 54.968	5.492 to 54.964
Index ranges	$-9 \le h \le 8$, $-12 \le k \le 12$, $-20 \le l \le 20$	$-15 \le h \le 15$, $-7 \le k \le 5$, $-19 \le l \le 17$
Reflections collected	10977	8078
Independent reflections	5033 [R_{int} = 0.0493, R_{sigma} = 0.0605]	3723 [R_{int} = 0.0290, R_{sigma} = 0.0407]
Data/restraints/parameters	5033/0/253	3723/1/264
Goodness-of-fit on F^2	1.038	1.023
Final R indexes [$I \ge 2\sigma$ (I)]	R_1 = 0.0369, wR_2 = 0.0789	R_1 = 0.0263, wR_2 = 0.0621
Final R indexes [all data]	R_1 = 0.0465, wR_2 = 0.0851	R_1 = 0.0282, wR_2 = 0.0633
Largest diff. peak/hole / e Å^{-3}	1.66/-1.56	1.34/-1.08
Flack parameter	/	-0.010(9)

Spectroscopic characterization of the studied azoles

Imidazole (im). MW = 68.06. IR (KBr, ν, cm^{-1}): 3124s (ν(N–H)), 3020s (ν($C_{diazole}$–H)), 1576m, 1542s, 1497m, 1448m (ν(C=C) and ν(C=N)), 842s, 757s, 738s, 660s, 620m (γ($C_{diazole}$–H)). ^{1}H NMR (200 MHz, DMSO-*d*$_6$): δ = 12.05 (*s*, 1H, NH), 7.64 (*s*, 1H, C2H), 7.01 (*s*, 2H, C4H and C5H). UV-Vis ($CHCl_3$, λ_{max}, nm): 260 ($\varepsilon = 2.2 \cdot 10^3$ $M^{-1}cm^{-1}$).

1-Isopropylimidazole (ipim). MW = 110.16. IR (KBr, *ν*, cm^{-1}): 3113m, 3044w, 3032w (*ν*($C_{diazole}$–H)), 2980s, 2935m (ν(C–H)), 1500s, 1460m, 1409m, 1373m (*ν*(C=C) and *ν*(C=N)), 917m, 818m, 739m, 667s, 643m (*γ*($C_{diazole}$–H)). ^{1}H NMR (200 MHz, DMSO-*d*$_6$): δ = 7.72 (*s*, 1H, C2H), 7.21 (*s*, 1H, C4H), 6.89 (*s*, 1H, C5H), 4.32 (*m*, C6H), 1.34 (*m*, 6H, C7H and C8H). UV-Vis ($CHCl_3$, λ_{max}, nm): 260 ($\varepsilon = 3.0 \cdot 10^3$ $M^{-1}cm^{-1}$).

1-Phenylimidazole (phim). MW = 144.17. IR (KBr, *ν*, cm^{-1}): 3116m, 3069m (ν($C_{diazole}$–H) and ν(C_{ar}–H)), 1601s, 1514s, 1505s, 1483m, 1461m (ν(C_{ar}=C_{ar}) and ν(C=N)), 817m, 760s, 692s, 659s (*γ*(C_{ar}–H) and *γ*($C_{diazole}$–H)). ^{1}H NMR (200 MHz, DMSO-*d*$_6$): δ = 8.30 (*s*, 1H, C2H), 7.77 (s, 1H, C4H), 7.66 (*m*, 2H, C7H and C11H), 7.52 (*m*, 2H, C8H and C10H), 7.36 (*m*, 1H, C9H), 7.13 ppm (*d*, *J* = 0.9 Hz, 1H, C5H). UV-Vis ($CHCl_3$, λ_{max}, nm): 262 ($\varepsilon = 3.5 \cdot 10^3$ $M^{-1}cm^{-1}$).

Clotrimazole (ctz). MW = 344.84. IR (KBr, *ν*, cm^{-1}): 3195w, 3167w, 3136w, 3112w (*ν*($C_{diazole}$–H) and *ν*(C_{ar}–H)), 2977w, 2916w, 2870w (*ν*(C–H)), 1585w, 1566w, 1493m, 1466m, 1443m, 1434m (*ν*(C_{ar}=C_{ar}) and *ν*(C=N)), 1211s, 1192w (*β*(C_{ar}–H) and *β*($C_{diazole}$–H)), 766vs, 753vs, 708s, 696m, 672s (*γ*(C_{ar}–H) and (γ($C_{diazole}$–H)), 634m (*ν*(C–Cl)). ^{1}H NMR (500 MHz, $CDCl_3$): δ = 7.46 (*d*, *J* = 5.6 Hz, 1H, C2H), 7.42 (*dd*, *J* = 7.9, 1.4 Hz, 1H, C8H), 7.33 (*m*, 7H, C10H, C14H, C15H, C16H, C20H, C21H, C22H), 7.26 (*m*, 1H, C9H), 7.19 (*m*, 4H, C13H, C17H, C19H, C23H), 7.05 (*m*, 1H, C4H), 6.92 (*dd*, *J* = 8.0, 1.6 Hz, 1H, C5H), 6.74 ppm (*t*, *J* = 1.3 Hz, 1H, C11H). UV-Vis ($CHCl_3$, λ_{max}, nm): 260 ($\varepsilon = 3.1 \cdot 10^3$ $M^{-1}cm^{-1}$).

Econazole (ecz). MW = 381.68. IR (KBr, ν, cm^{-1}): 3194w, 3176w, 3132w, 3115w, 3091w, 3064w (ν($C_{diazole}$–H) and ν(C_{ar}–H)), 2981w, 2969w, 2946w (ν(C–H)), 1590m, 1564m, 1505s, 1489s, 1473m, 1432m (ν(C_{ar}=C_{ar}) and ν(C=N)), 1233s, 1200m (*β*(C_{ar}–H) and *β*($C_{diazole}$–H), 1107s (*ν*(C–O)), 1090vs, 1046m, 1032m (*ν*(C_{ar}–Cl)), 800m, 787m, 733m, 661m, 626m (γ(C_{ar}–H)) and (γ($C_{diazole}$–H)). ^{1}H NMR (500 MHz, $CDCl_3$): *δ* = 9.02 (*s*, 1H, C2H), 7.48 (*d*, *J* = 1.8 Hz, 1H, C10H), 7.38 (*d*, *J* = 1.7 Hz, 1H, C4H), 7.35 (*d*, *J* = 1.8 Hz, 1H, C5H), 7.32 (*m*, 1H, C13H), 7.31 (*m*, 1H, C12H), 7.29 (*m*, 1H, C17H), 7.09 (*s*, 1H, H19), 7.08 (*s*, 1H, C16H), 7.01 (*t*, *J* = 1.6 Hz, 1H, C20H), 5.05 (*dd*, *J* = 7.8, 2.9 Hz, C7H), 4.51 (*d*, *J* = 11.8 Hz, 1H, C6H), 4.46 (*dd*, *J* = 14.4, 2.9 Hz, 1H, C6H), 4.36 (*dd*, *J* = 14.4, 7.8 Hz, 1H, C14H), 4.22 ppm (*d*, *J* = 11.8 Hz, 1H, C14H). UV-Vis ($CHCl_3$, λ_{max}, nm): 260 ($\varepsilon = 3.1 \cdot 10^3$ $M^{-1}cm^{-1}$).

Tioconazole (tcz). MW = 387.70. IR (KBr, *ν*, cm^{-1}): 3119w, 3094w, 3065w, 3023w (ν($C_{diazole}$–H) and ν(C_{ar}–H)), 2979w, 2935w (ν(C–H)), 1589m, 1562m, 1503s, 1467s, 1434m (ν(C_{ar}=C_{ar}) and ν(C=N)), 1230m, 1221m (*β*(C_{ar}–H) and *β*($C_{diazole}$–H)), 1120s (ν(C–O)), 828m, 815m, 785m, 692m (γ(C_{ar}–H)), 736vs (*ν*(C–S)), 628m (ν(C–Cl)). ^{1}H NMR (500 MHz, $CDCl_3$): *δ* = 7.43 (*d*, *J* =2.1 Hz, 2H, C2H, C10H), 7.33 (*d*, *J* = 8.4 Hz, 1H, C12H), 7.28 (*dd*, *J* = 8.4, 2.0 Hz, 1H, C17H), 7.05 (*d*, *J* = 5.7 Hz, 1H, C13H), 7.01(*s*, 1H, C9H), 6.88 (*s*, 1H, C5H), 6.75 (*d*, *J* =5.7 Hz, 1H, C4H), 4.94 (*dd*, *J* = 7.7, 2.7 Hz, 1H, C7H), 4.40 (*d*, *J* = 11.9 Hz, 1H, C14H), 4.24 (*d*, *J* = 11.9 Hz, 1H, C14H), 4.16 (*dd*, *J* = 14.5, 2.7 Hz, 1H, C6H), 4.00 ppm (*dd*, *J* = 14.5, 7.7 Hz, 1H, C6H). UV-Vis ($CHCl_3$, λ_{max}, nm): 262 ($\varepsilon = 1.3 \cdot 10^3$ $M^{-1}cm^{-1}$).

Voriconazole (vcz). MW = 349.31. IR (KBr, *ν*, cm^{-1}): 3196br (*ν*(O–H)), 3120w, 3047w, 3017w (*ν*($C_{triazole}$–H) and *ν*(C_{ar}–H)), 2995w, 2979w, 2941w (*ν*(C–H)), 1619s, 1587vs, 1507s, 1496vs, 1451vs, 1408vs (*ν*(C_{ar}=C_{ar}) and *ν*(C=N)), 1278s (*δ*(O–H)), 1249m, 1210m (*β*(C_{ar}–H) and *β*($C_{triazole}$–H)), 1132s (*ν*(C–F)), 1054m (*ν*(C–O)), 858s, 825w, 787w, 779m, 724m, 718m (*γ*(C_{ar}–

H)) and (γ($C_{triazole}$–H)), 622m (β(C_{ar}–F)). ^{1}H NMR (500 MHz, $CDCl_3$): δ = 8.93 (*t*, *J* = 3.7 Hz, 1H, C18H), 8.62 (*d*, *J* =1.4 Hz, 1H, C20H), 7.96 (*s*, 1H, C5H), 7.62 (*m*, 1H, C3H), 7.55 (*s*, 1H, C9H), 6.85 (*m*, 1H, C12H), 6.82 (*m*, 1H, C10H), 6.49 (*s*, 1H, OH), 4.72 (*d*, *J* = 14.2 Hz, 1H, C6H), 4.32 (*d*, *J* = 14.2 Hz, 1H, C6H), 4.13 (*q*, *J* = 7.1 Hz, 1H, C14H), 1.11 ppm (*d*, *J* = 7.1 Hz, 3H, C15H). UV-Vis ($CHCl_3$, λ_{max}, nm): 267 (ε = $2.3 \cdot 10^3$ $M^{-1}cm^{-1}$)